

Influence of Winding Structure and the Effect of MMF Harmonics to the Spindle Motor Performance for Ultrahigh TPI HDD

H. N. Phyu, N. L. H. Aung, and C. Bi

Data Storage Institute, A*STAR, 117608 Singapore

The technologies for maintaining high recording density to suppress mechanical vibration and media flutter for ultrahigh TPI hard disk drive (HDD) require advance spindle motor design and technology against the traditional norms. To realize multimagnetic poles with limited stator slots, spindle motors generally use concentrated windings which offer small end winding and simple structure suitable for mass production. There is a variety of ways to construct a motor with different winding structures based on different pole/slot combinations. Winding structures directly affect the producing of motor back-emf and torque which determine motor capacity, reliability and efficiency. In this work, detailed analysis is carried out to identify the optimal winding structures of the high speed spindle motor and analyze their effect on the motor performances by using magneto-motive force harmonics analysis and electromagnetic magnetic field analysis. Results are useful in preliminary and final optimal designs of the high speed spindle motors.

Index Terms—Concentrated winding structure, hard disk drive (HDD) spindle motor, magneto-motive force (MMF) harmonics analysis, motor winding layout.

I. INTRODUCTION

THE recording track density of the hard disk drive (HDD) is getting higher because of the continuous development in media, head, spindle motor and mechatronics technologies. Spindle motor is one of the key components in a disk drive system and, in many ways, determines drive capacity and reliability and performance. The technologies for maintaining high recording densities to suppress mechanical vibration and media flutter require advance spindle motor design and technology.

To realize the multimagnetic poles with limited stator slots, spindle motor generally used concentrated windings which offer small end windings, high efficiency and simple structure suitable for mass production. There is a variety of ways to construct various winding structures with the different combinations of slots and poles of the motor. Winding structures directly affect the producing of motor back-emf, torque and torque ripple which determine motor capacity, reliability and efficiency. Intensive research has been done by Hanselman [1], Cros [2] and Kocabas [3] for finding all possible winding structures by determining the highest value of winding factor (K_w) for permanent magnet (PM) machines with concentrated windings. This paper extends their findings to identify the optimal winding structures for a multimagnetic poles HDD spindle motor and the influence of their effects to the motor performances. Detailed analysis is done by magneto-motive force (MMF) harmonic analysis. The finite element method (FEM) is used to analyze the motor performances with different winding structures.

II. WINDING STRUCTURE IN SPINDLE MOTORS

Distributed winding structures are commonly used in electric machines with large power because the MMF waveform

Manuscript received November 30, 2012; revised February 04, 2013; accepted February 04, 2013. Date of current version May 30, 2013. Corresponding author: H. N. Phyu (e-mail: Hla_nu_phyu@dsi.a-star.edu.sg).

Color versions of one or more of the figures in this paper are available online at <http://ieeexplore.ieee.org>.

Digital Object Identifier 10.1109/TMAG.2013.2247389

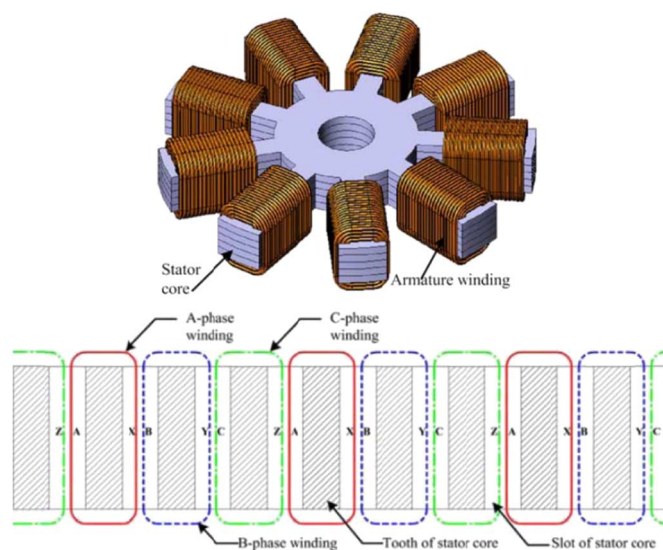


Fig. 1. Concentrated winding and winding layout for HDD spindle motor [4].

produced by the armature current of the distributed winding is close to sinusoidal which excessively reduce motor noise and vibration. However, the big space taken by the end winding of distributed winding structures is a constraint for space limited, compact structure HDD spindle motors. For utilizing the limited stator slots to realize multimagnetic pole-pair, concentrated windings are the most reliable winding structures for the HDD spindle motor.

Fig. 1 shows a typical balanced three-phase concentrated winding used in the spindle motor, where one coil is wound around one tooth of the stator core. There is no overlap between the end coils of adjacent windings. Three consecutive slots form one winding cycle. The distance between the centers of neighboring coils is 120 electrical degrees. The windings of the same phase are connected in series to obtain high torque constant. The three phase windings can be either Y-connected or Δ -connected.

Winding structures are directly related with the motor performances and determine the motor capacity, reliability and efficiency. Hence, to identify the optimal winding structure for the

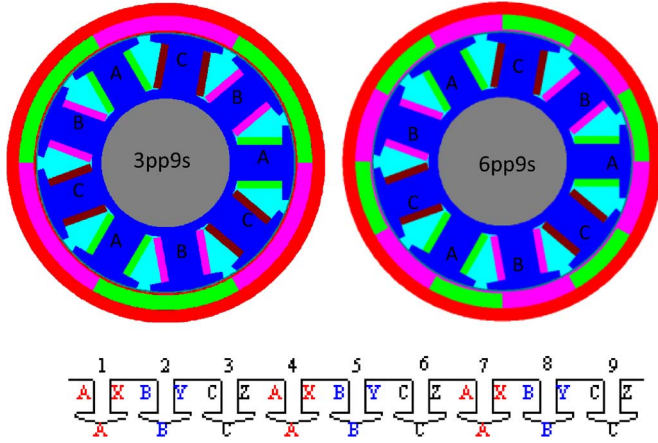


Fig. 2. Winding arrangement for 3pp9s and 6pp9s.

high performance spindle motor is essential in both preliminary design and final optimal design stages.

III. CONCENTRATED WINDING AND MMF HARMONICS

Current flowing through the armature windings produces the magnetic field. Interaction between the field produced by armature current and the rotor magnet generates electromagnetic (EM) torque. Alternatively, the interaction between the stator harmonic and the rotor harmonic with the same magnetic pole-pair generates the torque to operate the motor. Therefore, the pole-pair of the rotor magnet should match one of the harmonic fields generated by stator winding MMF.

The waveform of the stator winding MMF can be expressed by using the Fourier analysis as [4]

$$F_g(\theta) = \sum_{n=1}^{\infty} F_n \sin(n\theta). \quad (1)$$

The MMF generated by the stator winding is the sum of the MMF harmonics. The fundamental harmonic for phase A winding can be represented as

$$F_{a1}(\theta) = F_{p1} \sin(p\theta) = K i_a \sin(p\theta) \quad (2)$$

where p is the pole-pair of the motor, K is the constant determined by the number of winding turns and layout of the winding.

The winding current $i(t)$ varies with time and can be represented as

$$i_a(t) = I_m \sin(\omega t) \quad (3)$$

where ω is the angular frequency of the current. From (2) and (3) MMF waveform of the winding phase A can be represented as

$$\begin{aligned} F_{a1}(\theta) &= K I_m \sin(\omega t) \sin(p\theta) \\ &= \frac{K I_m}{2} [\cos(\omega t - p\theta) - \cos(\omega t + p\theta)]. \end{aligned} \quad (4)$$

TABLE I
POLE/SLOT COMBINATIONS AND CORRESPONDING WINDING STRUCTURES

3pp9s 6pp9s	4pp9s 5pp9s	7pp9s 2pp9s	8pp9s
ABCABCABC	AaABbBCcC	ABaCAcBCb	AAbCCaBBc

Hence, winding phase B and phase C can be represented as

$$F_{b1}(\theta) = K i_b \sin(p\theta - 120^\circ) \quad (5)$$

$$F_{c1}(\theta) = K i_c \sin(p\theta - 240^\circ). \quad (6)$$

If the currents i_b and i_c vary with time

$$i_b(t) = I_m \sin(\omega t - 120^\circ)$$

$$i_c(t) = I_m \sin(\omega t - 240^\circ). \quad (7)$$

Hence, the MMF generated by the three-phase winding is [4]

$$\begin{aligned} F_g(\theta, t) &= F_{a1}(\theta, t) + F_{b1}(\theta, t) + F_{c1}(\theta, t) \\ &= \frac{3K I_m}{2} \cos(\omega t - p\theta) = F_{m1} \cos(\omega t - p\theta). \end{aligned} \quad (8)$$

From (8), it is found that the summation of the triple MMF harmonics is zero for three-phase winding. Therefore, the effect of the triple MMF harmonics will not be included in energy conversion.

A. Determination of Winding Structures

For three-phase machines with balanced concentrated windings, possible combinations of poles and slots can be determined by [2]–[5]

$$\frac{s}{[GCD(s, pp)]} = 3k \quad (9)$$

where s is the number of slots, pp is the number of pole-pair, k is an integer number and GCD is greatest common divisor.

The number of slots per pole per phase S_{pp} is defined by

$$S_{pp} = \frac{s}{pp \cdot n} \quad (10)$$

where n is the number of phase. In this work, a nine-slot structure is used for analysis. Based on (9) and (10), a nine-slot structure can form nine combinations of poles/slots such as: 2pp9s, 3pp9s, 4pp9s, 5pp9s, 6pp9s, 7pp9s, 8pp9s, 10pp9s and 11pp9s (where pp is pole-pair and s is slot). Since the diameter of the PM ring of a spindle motor is very small (PM outer diameter is 24.85 mm and inner diameter 22.85 mm), it is difficult to magnetize to form 20 poles and 22 poles for 10pp9s and 11pp9s. Hence, these two combinations are omitted in this analysis. Apply the technique developed by Cros [2]; there would be four possible winding structures for 2pp9s, 3pp9s, 4pp9s, 5pp9s, 6pp9s, 7pp9s and 8pp9s as shown in Table I.

B. MMF Harmonics Analysis

MMFs generated by the stator winding are calculated for different winding layouts using magnetic circuit analysis. Fourier analysis as mentioned in Section II is carried out to analyze

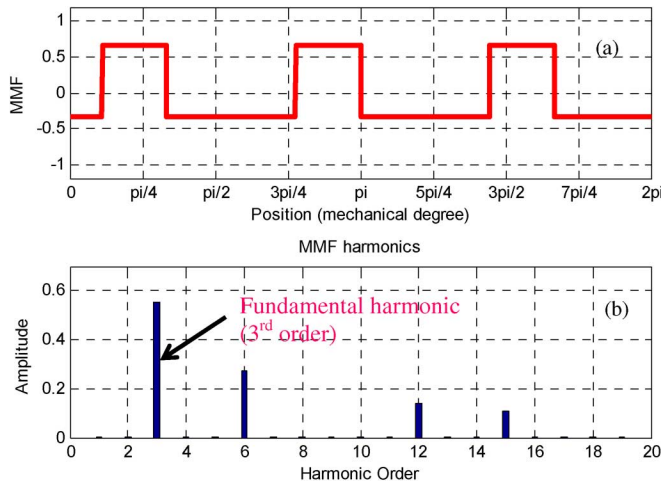


Fig. 3. MMF waveform and its harmonics for ABCABCABC winding structure. (a) MMF generated by Phase A winding. (b) Spectrum of MMF harmonics obtained by Fourier analysis.

the MMF harmonics. It is logical to select the fundamental harmonic of the stator winding MMF (which are normally the strongest) to match the rotor magnet pole-pair to generate the EM torque. However, this condition is not valid for all winding structures. Some winding structures generate subharmonics which are stronger than their fundamental harmonic. Detail analysis has been carried out with different winding structures as follows. In each winding arrangement, A and X represents the go and return side of Phase A winding, B and Y represents the go and return side of Phase B winding and C and Z represents the go and return side of Phase C winding, respectively.

1) *ABCABCABC Winding Structure*: In ABCABCABC winding structure, fundamental first harmonic (third order in space domain) is the strongest as shown in Fig. 3(b) and the rotor magnet can choose three pole-pairs. However, the number of pole-pairs of the rotor can increase if the next order harmonic field (sixth order in space domain) is selected to match the pole-pair of the PM ring. Therefore, for ABCABCABC winding structure, nine slots can form both three pole-pairs and six pole-pairs. Other higher order harmonics except the triple MMF harmonics can contribute to energy conversion, but their amplitudes are too small to take into account. Hence, for a nine-slot ABCABCABC winding structure, 3pp and 6pp are the most reliable pole-pairs to choose.

2) *AaABbBCcC Winding Structure*: In AaABbBCcC winding structure (Fig. 4), the fundamental space harmonic is low but its fourth order harmonic is the strongest as shown in Fig. 5. Hence, a rotor magnet is chosen as four pole-pairs. On the other hand, third order harmonic is the second strongest but it cannot contribute energy conversion for three-phase winding. Hence, its fifth harmonic is the next one to choose and it can form five pole-pairs for this winding structure.

3) *ABaCaBCbC Winding Structure*: In ABaCaBCbC winding structure, as shown in Figs. 6 and 7, third and sixth are the triple of the harmonic; therefore, they cannot be selected to match the pole-pair of PM ring. Only the fourth and seventh order harmonic can select. Therefore, the motor pole pair can form two pole-pairs and seven pole-pairs for that winding structure.

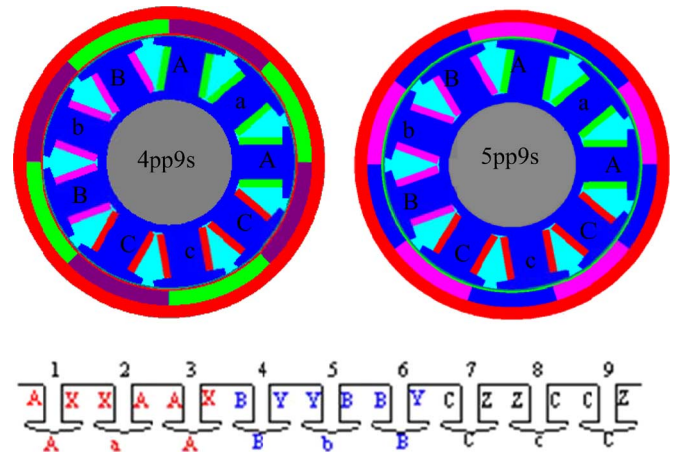


Fig. 4. Winding arrangement for 4pp9s and 5pp9s.

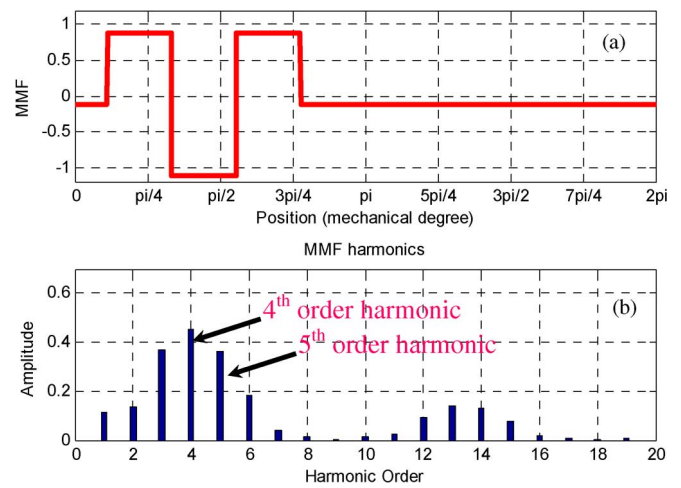


Fig. 5. MMF waveform and its harmonics for AaABbBCcC winding structure. (a) MMF generated by Phase A winding. (b) Spectrum of MMF harmonics obtained by Fourier analysis.

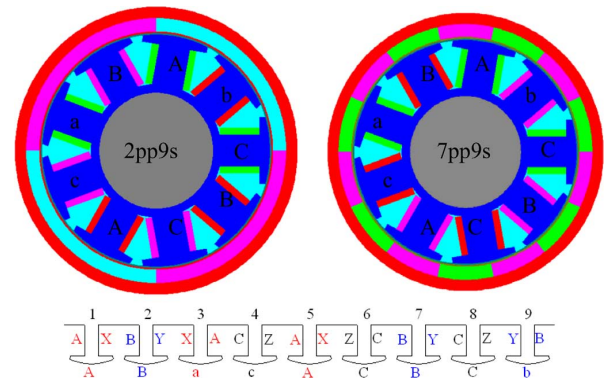


Fig. 6. Winding arrangement for 2pp9s and 7pp9s.

4) *AAbCCaBBc Winding Structure*: In AAbCCaBBc winding structure (Fig. 8), the eighth order harmonic is the most reliable because third harmonic cannot contribute to energy conversion for three-phase winding and the strongest first order fundamental harmonic cannot form a pole-pair. Fig. 9 shows MMF generated by Phase A winding for the AAbCCaBBc winding structure and spectrum of MMF harmonics obtained by Fourier analysis.

Stator MMF harmonics analysis shows that even if the only desired MMF component in normal operation is fundamental,

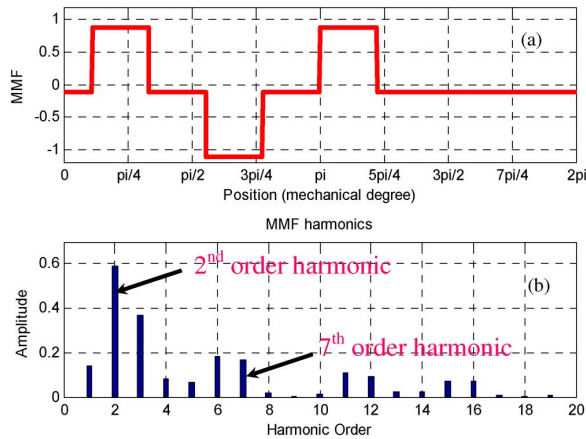


Fig. 7. MMF waveform and its harmonics for ABaCacBCb winding structure. (a) MMF generated by Phase A winding. (b) Spectrum of MMF harmonics obtained by Fourier analysis.

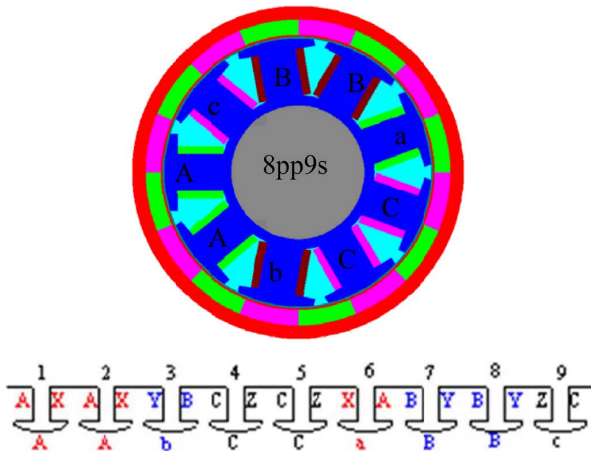


Fig. 8. Winding arrangement for 8pp9s.

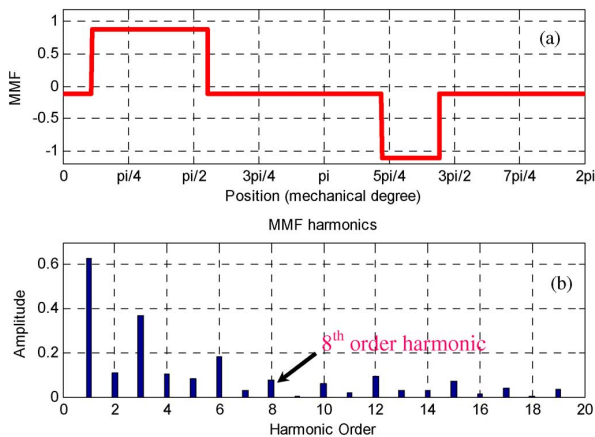


Fig. 9. MMF waveform and its harmonics for AAbCCaBBc winding structure. (a) MMF generated by Phase A winding. (b) Spectrum of MMF harmonics obtained by Fourier analysis.

there are subharmonics which are stronger than the fundamental. In such a condition, the strongest harmonic is selected to determine the pole-pair to produce the effective torque. In spindle motor design, one can select the second strongest, high order harmonic to form pole-pair in most of the conditions. High order harmonic can increase pole-pairs so that they increase the number of pulsation of the cogging torque which

TABLE II
MOTOR SPECIFICATIONS

Rotor outer diameter	24.85mm
Rotor inner diameter	22.85mm
Stator outer diameter	20.0 mm
Magnet thickness	1.15mm
Air gap	0.275mm
Rated speed	15000rpm
Permanent magnet	NdFeB

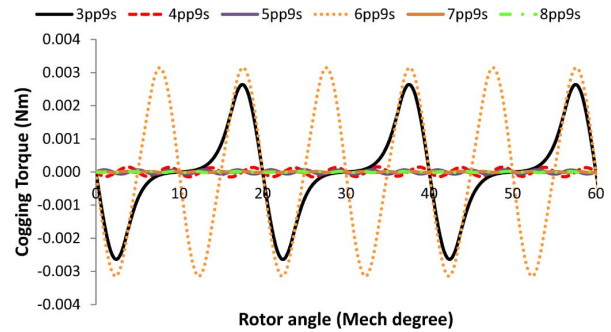


Fig. 10. Cogging torque for 3pp9s, 4pp9s, 5pp9s, 6pp9s, 7pp9s and 8pp9s.

is one of the concerns in spindle motor design. The number of pulsations of the cogging torque is derived from the least common multiple (LCM) of slots and poles. LCM value should be as high as possible since the LCM value equals the number of cogging periods per rotor revolution [6]. Higher cogging frequency results in lower magnitude. The compromise can increase eddy current loss because of high frequency [7].

IV. PERFORMANCE ANALYSIS OF MOTOR WITH DIFFERENT WINDING STRUCTURES

Motor performance are analyzed based on possible winding structures shown in Section III. Motor dimensions are the same for each structure, except the winding arrangements and magnetic pole-pairs are different. Motor specifications are listed in Table II. For a permanent magnet (PM), bonded NdFeB with energy product 10 MGOe is used. Radial PM magnetization is used in this analysis as it is the most common type of PM excitation and widely used in most of the high speed motors.

A. Cogging Torque

The cogging torque can cause startup problems and greatly effect the running torque fluctuation. Hence, it is desirable to minimize it at the design stage. Motor cogging torque with different pole/slots combinations is calculated by FEM using the Virtual Work Method. Results are shown in Fig. 10. 3pp9s and 6pp9s, which share the same winding structure of ABCABC, have very high cogging torque compared with other structures as shown in Fig. 10. 7pp9s and 8pp9s have the lowest cogging torques as shown in Fig. 11. The LCM of 7pp9s and 8pp9s are the highest among the other pole/slot combinations. Results show that a motor with different winding structure forms different rotor pole-pairs and it directly effects the generation of cogging torques.

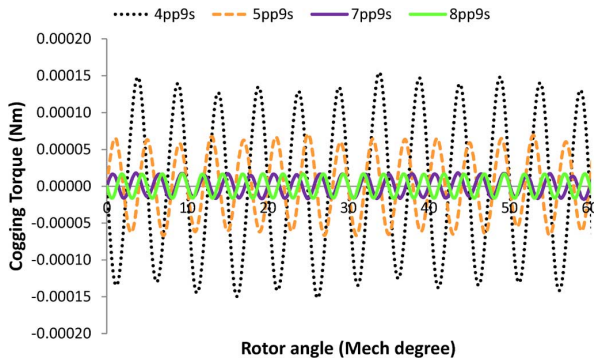


Fig. 11. Comparison of cogging torque for 4pp9s, 5pp9s, 7pp9s and 8pp9s.

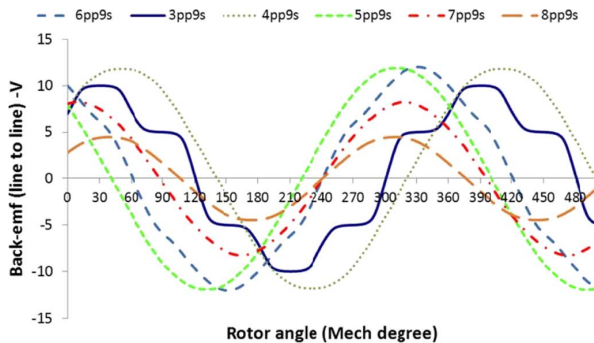


Fig. 12. Back-emf waveform for 3pp, 4pp, 5pp, 6pp, 7pp and 8pp nine-slot motor with different winding structures.

B. Back-emf

For a high efficiency, good quality high speed machines, the back-emf waveform induced by rotor motion must be well estimated because it is closely related to the producing of EM torque and torque ripple of the motor [8]. Motor designers want to get purely sinusoidal or trapezoidal back-emf waveform based on motor types and control schemes. Even though it is theoretically possible to produce smooth torque for any back-emf waveform by controlling the current waveform with a chopping scheme, this requires a relatively complex and precise control procedure and expensive electronic circuits.

HDD spindle motors are normally driven by voltage source inverter in BLDC mode. Commutation takes place between every 60 electrical degrees. Hence for the ideal case, a motor has to be designed for trapezoidal back-emf for BLDC drive. However, it is difficult to implement trapezoidal back-emf for a spindle motor which has very limited stator slots to realize multiple magnetic poles. Therefore, sinusoidal back-emf is commonly used in most of the commercial HDD spindle motors to simplify the quality control procedure which is very important in mass production [9]. This is not an optimal way to drive spindle motor with sinusoidal back-emf in BLDC drive mode but it can greatly reduce the manufacturing cost and less dependence on high power DSP, yet satisfactory performance.

In this work, motor back-emf with different winding structures are calculated by FEM. Simulated results of line to line back-emf are as shown in Fig. 12. Results show that winding structure AaABbBCcC belongs to 4pp9s and 5pp9s, winding structure ABaCaBCb belongs to 7pp9s motor and winding structure AAbCCaBBc belongs to 8pp9s. The motor generates sinusoidal back-emf as shown in Fig. 13, resulting in lower

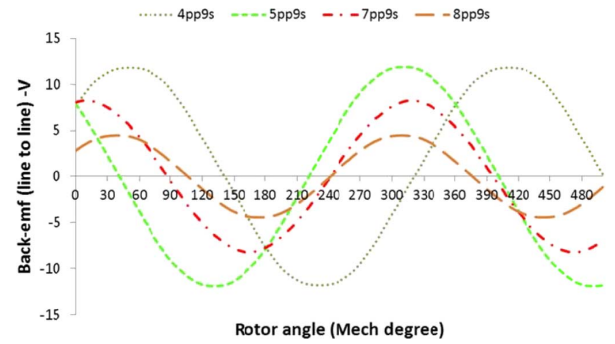


Fig. 13. Sinusoidal back-emf produced by 4pp9s, 5pp9s, 7pp9s and 8pp9s with different winding structures.

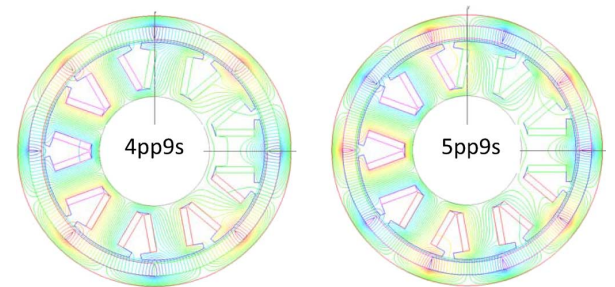


Fig. 14. Magnetic field distribution of the 4pp9s and 5pp9s motors.

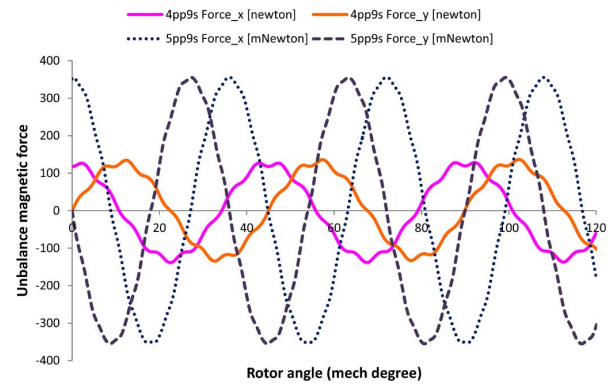


Fig. 15. UMP for 4pp9s and 5pp9s motors.

torque ripple. Among them, 4pp9s and 5pp9s which share the same winding structure of AaABbBCcC has the highest back-emf in magnitude. In turn, the torque constant would be the highest and motor efficiency will be the highest among other structures. Based on analysis, it can be concluded that winding structures determine both wave shapes and magnitudes of the back-emf which directly effect the producing of motor torque, torque ripple and torque constant and determine motor efficiency and capacity.

C. Unbalance Magnetic Pull (UMP)

Winding structures AaABbBCcC, ABaCaBCb and AAbCCaBBc generate favorable low cogging torque and sinusoidal back-emf for spindle motor; however, these structures produce unbalanced magnetic pull. Fig. 14 shows magnetic field distribution of 4pp9s and 5pp9s where left side and right side of the field are not balanced and it produces UMP without the rotor eccentricity. Calculated UMP for 4pp9s, 5pp9s, 7pp9s and 8pp9s are shown in Figs. 15 and 16. Comparison of magnitude of UMP is shown in Fig. 17. 5pp9s, 7pp9s and 8pp9s motors have very

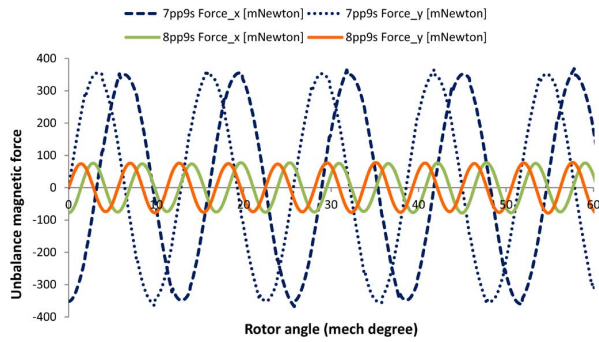


Fig. 16. UMP for 7pp9s and 8pp9s motors.

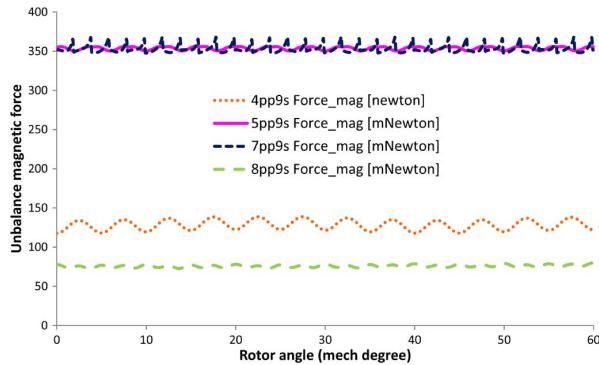


Fig. 17. Comparison of magnitude of UMP for 4pp9s, 5pp9s, 7pp9s and 8pp9s with different winding structures.

low UMP compared with 4pp9s. The UMP is one of the main sources of acoustic noise and vibration in the motor operation [10]. A good design spindle motor must have very low or no UMP. To reduce UMP even without the rotor eccentricity, it is necessary to analyze the effect of the winding structure and rotor magnetic pole-pair to UMP in the preliminary design stage to avoid unwanted noise and vibration.

V. DISCUSSION AND CONCLUSION

In this work, MMF harmonic analysis is carried out to identify the motor pole-pairs with different winding structures. The placement of concentrated windings and the influence of winding configurations on motor torque, back-emf, cogging torque, and UMP are investigated. Based on motor performance analysis using different winding structures, the advantages and disadvantages of different structures can be clarified and the reasonable winding structures can thus be determined for the specific application and the practical operating requirements of the motor.

Ultrahigh TPI HDD application requires very low acoustic noise and vibration, high reliability, low cost, constant torque, high speed, and a high efficiency motor to execute error free read/write operation. As mentioned in Section IV, most of the commercial HDD spindle motors operate in BLDC mode with sinusoidal back-emf to reduce torque ripple, with less dependence on capacity of DSP, to reduce manufacturing cost and to simplify the quality control procedure in mass production.

In this work, motor performance is analyzed based on possible winding structures by using FEM. Results show that winding structures AaABbBCcC, ABaCaCbC and AAbCCaBBc generate favorable low cogging torque and sinusoidal back-emf for spindle motor. Among them, 8pp9s motor with AAbCCaBBc winding structure generates the lowest cogging torque and UMP; however, back-emf is the lowest which means the motor torque constant would be the lowest and motor efficiency would be the lowest which is the unfavorable condition for ultrahigh TPI application. For obvious reasons, efficiency of the spindle motor must be high, since the efficiency refers to not only low power consumption but also low heat production. This is important for the product life and reliability of the HDD. Again, 4pp9s and 5pp9s which share the same winding structure of AaABbBCcC have the highest back-emf in magnitude. In turn, the torque constant would be the highest and motor efficiency will be the highest among other structures. In addition, 5pp9s motor has lower cogging torque and UMP compared with 4pp9s. Therefore, 5pp9s motor with AaABbBCcC structure is the most promising one to produce the highest torque constant and the highest motor efficiency with reasonable noise and vibration for this particular application.

Based on the detailed analysis of motor performances with different winding structures, it can be concluded that to improve the motor design, efficiency and reliability, applying the correct winding structure with an appropriate pole/slot combination is important based on desired applications. Preliminary investigation of the effect of winding structures of the motor is essential to get the motor's optimal performance.

REFERENCES

- [1] D. Hanselman, *Brushless Permanent Magnet Motor Design*, 2nd ed. New York, NY, USA: McGraw-Hill, 2006.
- [2] J. Cros and P. Viarouge, "Synthesis of high performance PM motors with concentrated windings," *IEEE Trans. Energy Convers.*, vol. 17, no. 2, pp. 248–253, Jun. 2002.
- [3] D. A. Kocabas, "Novel winding and core design for maximum reduction of harmonic magnetomotive force in AC motors," *IEEE Trans. Magn.*, vol. 45, no. 2, pp. 735–746, Feb. 2009.
- [4] A. A. Mamum, G. X. Guo, and B. Chao, *Hard Disk Drive Mechatronics and Control*. London, U.K.: Taylor & Francis, 2007, pp. 219–224.
- [5] C. C. Hwang, S. P. Cheng, and C. M. Chang, "Design of high performance spindle motors with concentrated windings," *IEEE Trans. Magn.*, vol. 41, no. 2, Feb. 2005.
- [6] F. Magnussen and H. Lendenmann, "Parasitic effects in PM machines with concentrated windings," *IEEE Trans. Ind. Appl.*, vol. 43, no. 5, pp. 1223–1231, Sep. 2007.
- [7] J. Li, D. W. Choi, D. H. Son, and Y. H. Cho, "Effects of MMF harmonics on rotor eddy-current losses for inner-rotor fractional slot axial flux permanent magnet synchronous machines," *IEEE Trans. Magn.*, vol. 48, no. 2, pp. 839–842, Feb. 2012.
- [8] J. H. Lee, D. H. Kim, and I. L. H. Park, "Minimization of higher back-emf harmonics in permanent magnet motor using shape design sensitivity with B-spline parameterization," *IEEE Trans. Magn.*, vol. 39, no. 3, pp. 1269–1272, May 2003.
- [9] J. H. Walker, *Large Synchronous Machines: Design, Manufacture and Operation*. Oxford, U. K.: Oxford Univ. Press, 2001.
- [10] J. H. Lee, D. H. Kim, and I. L. H. Park, "Minimization of higher back-emf harmonics in permanent magnet motor using shape design sensitivity with B-spline parameterization," *IEEE Trans. Magn.*, vol. 39, no. 3, pp. 1269–1272, May 2003.